

Collisionless and hydrodynamic excitations of trapped boson-fermion mixtures

Xia-Ji Liu^{1,2} and Hui Hu^{3,4}

¹*European Laboratory for Nonlinear Spectroscopy and Dipartimento
di Fisica,*

Università di Firenze, Via Nello Carrara 1, 50019 Sesto Fiorentino, Italy

²*Institute of Theoretical Physics, Academia Sinica, Beijing 100080, China*

³*Abdus Salam International Center for Theoretical Physics, P. O. Box 586,
Trieste 34100, Italy*

⁴*Department of Physics, Tsinghua University, Beijing 100084, China*

(November 1, 2018)

Abstract

Within a scaling ansatz formalism plus Thomas-Fermi approximation, we investigate the collective excitations of a harmonically trapped boson-fermion mixture in the collisionless and hydrodynamic limit at low temperature. Both the monopole and quadrupole modes are considered in the presence of spherical as well as cylindrically symmetric traps. In the spherical traps, the frequency of monopole mode coincides in the collisionless and hydrodynamic regime, suggesting that it might be undamped in all collisional regimes. In contrast, for the quadrupole mode, the frequency differs largely in these two limits. In particular, we find that in the hydrodynamic regime the quadrupole oscillations with equal bosonic and fermionic amplitudes generate an exact eigenstate of the system, regardless of the boson-fermion interaction. This resembles the Kohn mode for the dipole excitation. We discuss in some detail the behavior of monopole and quadrupole modes as a function of boson-

fermion coupling at different boson-boson interaction strength. Analytic solutions valid at weak and medium fermion-boson coupling are also derived and discussed.

PACS numbers:03.75.Fi, 05.30.Fk, 67.60.-g

I. INTRODUCTION

Shortly after the achievement of Bose-Einstein condensation of dilute, magnetically trapped alkali atoms [1,2], the investigation of collective excitations in these systems has become a very active research field (see [3] for a recent theoretical review). The high accuracy of frequency measurements and the sensitivity of collective phenomena to interaction effects makes them good candidates to unravel the dynamical correlation of the many-body system. So far, experimental results have been obtained for low-lying collective modes of a trapped condensate in a wide temperature regime, including breathing modes [4], surface modes [5], and the scissors mode [6]. These experiments have in turn stimulated a considerable amount of theoretical work.

Recently the quantum degenerate regime has also been reached in a magnetically trapped Fermi gas [7], and in a mixture of Bose and Fermi particles [8,9]. The latter system is in particular interesting since it serves as one typical example in which the intermingled particles obey different statistics. Up to date the static property [10,11,12,13], the phase diagram and phase separation [14,15,16], stability conditions [17,18] and collective excitations [19,20,21,22,23,24,25,26] of trapped boson-fermion mixtures have been theoretically investigated. In a recent experiment, the collapse of a degenerated Fermi gas caused by the strong attractive interaction with a Bose-Einstein condensate has been observed in an atomic mixture of ^{40}K – ^{87}Rb [27], and measurements of collective excitations might be available soon also in such systems.

The purpose of the present paper is to study the collective excitations of magnetically trapped boson-fermion binary mixtures in two different regimes: a collisionless regime where the collision rate is small compared with the frequencies of particle motion in the trap and a hydrodynamic (collisional) regime in which collisions are sufficiently strong to ensure local thermodynamic equilibrium. From the experimental point of view the temperature T of all the realized boson-fermion mixtures is around the Fermi temperature T_F (more precisely, $T \geq 0.2T_F$ [8]), and the systems are possibly in or close to the hydrodynamic regime, since

the sympathetic cooling technique used in the experiments usually requires a large boson-fermion interaction strength so that the frequent collisions between fermions and bosons can foster the local thermal equilibrium and ensure efficient thermalization of the fermionic component to reach the quantum degeneracy. Of course, as far as the strongly degenerate regime (where $T \ll T_F$) is concerned, the collisions are rare because of Fermi statistic, and the systems will be finally in the collisionless regime.

Several theoretical analysis have already been presented for the collective excitations of a *spherically* trapped boson-fermion mixture. The collisionless modes are considered by a sum-rule approach [24] or in the random-phase approximation [25,26]. The collisional collective oscillations are discussed by Minguzzi and Tosi [23], however, limited to the surface modes at weak fermion-boson coupling. On the other hand, the *homogeneous* boson-fermion mixtures have also been analytically studied [19,20,21,22]. The repulsion between the Bogoliubov phonon mode and zero-sound mode [19] (or Anderson mode [20]), is predicted when the degenerated Fermi gas is in the normal collisionless limit (or in the superfluid phase).

In this paper, we shall analyze systematically the collisionless and hydrodynamic monopole and quadrupole modes in the presence of spherical as well as cylindrically symmetric traps [28]. We discuss in some detail the behavior of those modes against boson-fermion coupling at different boson-boson interaction strength. In the spherical traps, we find that the monopole frequency coincides in the collisionless regime and in the hydrodynamic one, suggesting that it might be undamped in all collisional regimes. In contrast, for the quadrupole mode the frequency differs dramatically in these two limits. In particular, in the hydrodynamic regime the quadrupole oscillations with equal bosonic and fermionic amplitudes are found to generate an exact eigenstate of the system, resembling the Kohn mode for the dipole excitation. Analytic solutions valid at weak and medium fermion-boson coupling are also deduced and discussed.

The content of the paper is as follows. In the next section we derive equations of the low-energy collective excitation of a boson-fermion mixture in the Thomas-Fermi approximation by means of a scaling ansatz. In Sec. III we first briefly describe the parameters and

the numerical procedure employed in the present calculation. We then turn to detailed discussion of the results obtained by analyzing the dependence of the mode frequencies on the boson-fermion coupling and boson-boson interaction strength, the ground-state density distributions, and the mixing between bosonic and fermionic collective oscillations. The last section is devoted to summary and conclusions.

II. FORMULATION

We consider a dilute spin-polarized boson-fermion mixture trapped in a cylindrically symmetric harmonic oscillator potential at low temperature. In the semi-classical Thomas-Fermi approximation, the normal Fermi gas evolves according to the Boltzmann-Vlasov kinetic equation [29,30] (see the Eq. (2) below). In the collisionless regime, the collisions are rare and we can safely neglect the collision term (I_{coll}) that accounts for the damping of collective modes. On the opposite of the hydrodynamic regime, the collision term dominates and we resort to the Euler equation of motion [31], which can be deduced from Boltzmann-Vlasov kinetic equation under the assumption of local equilibrium for fermions [32]. For the bosonic part, we shall apply the same Stringari's hydrodynamic formulation [33] in both regimes, since the dynamics of the condensate is less affected by the collisions [34].

A. collisionless regime

According to the Stringari's hydrodynamic description [33], the low-energy dynamics of the trapped bosonic atoms is determined by the equations,

$$\begin{aligned} \frac{\partial n_b}{\partial t} + \nabla \cdot (\mathbf{v}_b n_b) &= 0, \\ m_b \frac{\partial \mathbf{v}_b}{\partial t} + \nabla \cdot \left(V_{ho}^b + g_{bb} n_b + g_{bf} n_f + \frac{1}{2} m_b \mathbf{v}_b^2 \right) &= 0, \end{aligned} \quad (1)$$

where $V_{ho}^b(\mathbf{r}) = \frac{1}{2} m_b (\omega_{\perp b}^2 \rho^2 + \omega_{zb}^2 z^2)$ is the cylindrical symmetric confining potential, and $n_b(\mathbf{r}, t)$, $n_f(\mathbf{r}, t)$ and $\mathbf{v}_b(\mathbf{r}, t)$ are the boson, fermion density and velocity field, respectively. The mean-field term $g_{bf} n_f(\mathbf{r}, t)$ is included to take into account the effect of boson-fermion

interaction [10]. The boson-boson and boson-fermion interaction strength for the pseudopotentials, g_{bb} and g_{bf} , are related to the s -wave scattering lengths a_{bb} and a_{bf} through $g_{bb} = 4\pi\hbar^2 a_{bb}/m_b$, $g_{bf} = 2\pi\hbar^2 a_{bf}/m_{bf}$ where $m_{bf} = m_b m_f / (m_b + m_f)$ is the reduced boson-fermion mass. In Eq. (1), we have already neglected the quantum kinetic energy pressure term $\frac{\hbar^2}{2m_b\sqrt{n_b}}\nabla^2\sqrt{n_b}$ in the spirit of the Thomas-Fermi approximation [3].

For the fermionic part in the collisionless regime, in order to take into account the effects of the boson-fermion interactions, we consider the mean-field description based on the Boltzmann-Vlasov kinetic equation [29,30] without the collisional term (I_{coll}),

$$\frac{\partial f}{\partial t} + \mathbf{v}_f \cdot \frac{\partial f}{\partial \mathbf{r}} - \frac{1}{m_f} \frac{\partial V_{ho}^f}{\partial \mathbf{r}} \cdot \frac{\partial f}{\partial \mathbf{v}_f} - \frac{g_{bf}}{m_f} \frac{\partial n_b}{\partial \mathbf{r}} \cdot \frac{\partial f}{\partial \mathbf{v}_f} = 0, \quad (2)$$

where $f(\mathbf{r}, \mathbf{v}_f, t)$ is the single particle phase space distribution function for fermions, $n_f(\mathbf{r}, t) = \int d^3\mathbf{v}_f f(\mathbf{r}, \mathbf{v}_f, t)$ and $V_{ho}^f(\mathbf{r}) = \frac{1}{2}m_f(\omega_{\perp f}^2 \rho^2 + \omega_{zf}^2 z^2)$ is the confining potential. The last term in the left hand side of Eq. (2) is a Hartree-Fock mean-field term, also known as the Vlasov contribution. The fermion-fermion interaction has been neglected as the polarized system is considered [35].

Without the boson-fermion interaction ($g_{bf} = 0$), both the Eqs. (1) and (2) admit the simple scaling solution, i.e.,

$$\begin{aligned} n_b(\mathbf{r}, t) &= \frac{1}{\prod_j b_j(t)} n_b^0\left(\frac{r_i}{b_i(t)}\right), \\ v_{bi}(\mathbf{r}, t) &= \frac{1}{b_i(t)} \frac{db_i(t)}{dt} r_i, \end{aligned} \quad (3)$$

for bosons [31,36] and

$$\begin{aligned} f(\mathbf{r}, \mathbf{v}_f, t) &= f_0\left(\frac{r_i}{\gamma_i(t)}, \tilde{\mathbf{v}}_f(\mathbf{r}, t)\right), \\ \tilde{\mathbf{v}}_{fi}(\mathbf{r}, t) &= \gamma_i(t) v_{fi} - \frac{d\gamma_i(t)}{dt} r_i, \end{aligned} \quad (4)$$

for fermions [29,30,37]. Here n_b^0 and f_0 are the equilibrium distributions. The dependence on time t is entirely contained the six scaling parameters, $b_i(t)$ and $\gamma_i(t)$, where $i = x, y$, and z . By substituting this solution into Eqs. (1) and (2), it is easily to show that, the scaling parameters obey the coupled differential equations [36,37],

$$\ddot{b}_i(t) + \omega_{ib}^2(t)b_i(t) - \frac{\omega_{ib}^2(0)}{b_i(t) \prod_j b_j(t)} = 0, \quad (5)$$

$$\ddot{\gamma}_i(t) + \omega_{if}^2(t)\gamma_i(t) - \frac{\omega_{if}^2(0)}{\gamma_i^3(t)} = 0. \quad (6)$$

Solutions of Eqs. (5) and (6) determine the evolution of both the boson and fermion density. In particular, the eigenfrequencies of small oscillations with $\omega_i(t) = \omega_i(0)$ are the resonance frequencies of the collective density (shape) oscillations under the weak perturbation of the external field. After linearizing around the equilibrium values $b_i = 1$ and $\gamma_i = 1$, one finds, in the case of the spherical harmonic traps, the result: $\omega_{Mb} = \sqrt{5}\omega_b$, $\omega_{Qb} = \sqrt{2}\omega_b$ and $\omega_{Mf} = 2\omega_f$, $\omega_{Qf} = 2\omega_f$ for the frequencies of the monopole and quadrupole oscillations, respectively, which is already well known in the literatures.

In the presence of the boson-fermion interaction ($g_{bf} \neq 0$), however, the simple scaling solution is no longer satisfied at every position \mathbf{r} after the substitution. A useful approximation, in the first order of g_{bf} , is to assume the scaling form of the solution as a priori, and fulfill it on average by integrating over the spatial coordinates. The same strategy has been recently used by Guery-Odelin [29] to investigate the effect of the interaction on the collective oscillation of a classical gas in the collisionless regime and by Menotti *et al.* to study the expansion of an interacting Fermi gas [30]. In the latter, the authors showed that the frequencies of the monopole and quadrupole modes for isotropic traps deduced in this approximation coincide with the result derived earlier by using the sum-rule approach. Of course, the assumption of the scaling ansatz is only meaningful for the small value of $|g_{bf}|$. It will apparently break down for a large and positive g_{bf} , at which the phase separation occurs.

In the approximation specified above, we substitute the scaling ansatz Eq. (3) into Stringari's hydrodynamic equations. By setting $R_i = r_i/b_i(t)$, one finds,

$$\begin{aligned} \ddot{b}_i(t)R_i + \omega_{ib}^2(t)b_i(t)R_i + \frac{g_{bb}}{m_b} \frac{1}{b_i(t) \prod_j b_j(t)} \frac{\partial n_b^0(\mathbf{R})}{\partial R_i} \\ + \frac{g_{bf}}{m_b} \frac{1}{b_i(t) \prod_j \gamma_j(t)} \frac{\partial n_f^0(\frac{b_i(t)}{\gamma_i(t)}R_i)}{\partial R_i} = 0, \end{aligned} \quad (7)$$

which reduces to the following form in equilibrium state,

$$\omega_{ib}^2(t)R_i + \frac{g_{bb}}{m_b} \frac{\partial n_b^0(\mathbf{R})}{\partial R_i} + \frac{g_{bf}}{m_b} \frac{\partial n_f^0(\mathbf{R})}{\partial R_i} = 0. \quad (8)$$

The equations for the scaling parameters $b_i(t)$ can be obtained by multiplying Eq. (7) by $R_i n_b^0(R_i)$ on both sides and integrating over the spatial coordinates. Making use of the equilibrium properties of the density distribution (8), after some straightforward algebra one finds,

$$\begin{aligned} \ddot{b}_i(t) + \omega_{ib}^2(t)b_i(t) - \frac{\omega_{ib}^2(0)}{b_i(t) \prod_j b_j(t)} \\ + \frac{g_{bf}}{m_b N_b \langle R_i^2 \rangle_b} \frac{1}{b_i \prod_j b_j} \int d^3 \mathbf{R} \frac{\partial n_f^0(\mathbf{R})}{\partial R_i} R_i n_b^0\left(\frac{\gamma_i}{b_i} R_i\right) \\ - \frac{g_{bf}}{m_b N_b \langle R_i^2 \rangle_b} \frac{1}{b_i \prod_j b_j} \int d^3 \mathbf{R} \frac{\partial n_f^0(\mathbf{R})}{\partial R_i} R_i n_b^0(\mathbf{R}) = 0, \end{aligned} \quad (9)$$

where $\langle R_i^2 \rangle_b = \frac{1}{N_b} \int d^3 \mathbf{R} n_b^0(\mathbf{R}) R_i^2$ is the average size of bosons along the i -axis. The last two terms in Eq. (9), linear in g_{bf} , account for the effects of boson-fermion interaction.

Analogous procedure can also be applied for the fermionic part [38]. The equations for the scaling parameters $\gamma_i(t)$ are finally found to take the form,

$$\begin{aligned} \ddot{\gamma}_i(t) + \omega_{if}^2(t)\gamma_i(t) - \frac{\omega_{if}^2(0)}{\gamma_i^3(t)} \\ + \frac{g_{bf}}{m_f N_f \langle R_i^2 \rangle_f} \frac{1}{\gamma_i \prod_j \gamma_j} \int d^3 \mathbf{R} \frac{\partial n_b^0(\mathbf{R})}{\partial R_i} R_i n_f^0\left(\frac{b_i}{\gamma_i} R_i\right) \\ - \frac{g_{bf}}{m_f N_f \langle R_i^2 \rangle_f} \frac{1}{\gamma_i^3} \int d^3 \mathbf{R} \frac{\partial n_b^0(\mathbf{R})}{\partial R_i} R_i n_f^0(\mathbf{R}) = 0, \end{aligned} \quad (10)$$

where $\langle R_i^2 \rangle_f = \frac{1}{N_f} \int d^3 \mathbf{R} n_f^0(\mathbf{R}) R_i^2$.

The coupled set of differential equations (9) and (10) is a generalization of Eqs. (5) and (6) in the presence of the boson-fermion coupling. It determines the dynamics of boson-fermion mixtures in the collisionless regime as far as the assumption of the simple scaling solution is valid. We shall only be interested in the small oscillation around the equilibrium state ($b_i, \gamma_i \approx 1$) and apply it to study the behavior of monopole and quadrupole modes against boson-fermion coupling. In this case, one can simplify the set of differential equations by expanding

$$\begin{aligned}
n_b^0\left(\frac{\gamma_i}{b_i}R_i\right) &\approx n_b^0(\mathbf{R}) + \sum_j \frac{\partial n_b^0(\mathbf{R})}{\partial R_j} \left(\frac{\gamma_j}{b_j} - 1\right) R_j, \\
n_f^0\left(\frac{b_i}{\gamma_i}R_i\right) &\approx n_f^0(\mathbf{R}) + \sum_j \frac{\partial n_f^0(\mathbf{R})}{\partial R_j} \left(\frac{b_j}{\gamma_j} - 1\right) R_j,
\end{aligned} \tag{11}$$

to obtain

$$\begin{aligned}
\ddot{b}_i(t) + \omega_{ib}^2(t)b_i(t) - \frac{\omega_{ib}^2(0)}{b_i(t) \prod_j b_j(t)} \\
+ \sum_k \frac{\omega_{ib}^2(0)B_{ik}}{b_i \prod_j b_j} \left(\frac{\gamma_k}{b_k} - 1\right) = 0,
\end{aligned} \tag{12}$$

and

$$\begin{aligned}
\ddot{\gamma}_i(t) + \omega_{if}^2(t)\gamma_i(t) - \frac{\omega_{if}^2(0)}{\gamma_i^3(t)} + \omega_{if}^2(0)F_i \left(\frac{1}{\gamma_i \prod_j \gamma_j} - \frac{1}{\gamma_i^3}\right) \\
+ \sum_k \frac{\omega_{if}^2(0)D_{ik}}{\gamma_i \prod_j \gamma_j} \left(\frac{b_k}{\gamma_k} - 1\right) = 0,
\end{aligned} \tag{13}$$

where

$$\begin{aligned}
B_{ik} &= \frac{g_{bf}}{m_b \omega_{ib}^2(0) N_b \langle R_i^2 \rangle_b} \int d^3 \mathbf{R} \frac{\partial n_f^0(\mathbf{R})}{\partial R_i} R_i R_k \frac{\partial n_b^0(\mathbf{R})}{\partial R_k}, \\
F_i &= \frac{g_{bf}}{m_f \omega_{if}^2(0) N_f \langle R_i^2 \rangle_f} \int d^3 \mathbf{R} \frac{\partial n_b^0(\mathbf{R})}{\partial R_i} R_i n_f^0(\mathbf{R}), \\
D_{ik} &= \frac{g_{bf}}{m_f \omega_{if}^2(0) N_f \langle R_i^2 \rangle_f} \int d^3 \mathbf{R} \frac{\partial n_b^0(\mathbf{R})}{\partial R_i} R_i R_k \frac{\partial n_f^0(\mathbf{R})}{\partial R_k},
\end{aligned}$$

are the dimensionless parameters proportional to g_{bf} . In the case of a cylindrical trap, those parameters can be reduced to $B_{\alpha\beta}$, F_α , and $D_{\alpha\beta}$ ($\alpha, \beta = \rho$ or z) in terms of the cylindrical coordinates, whose expressions are given in Appendix.

By linearizing Eqs. (12) and (13) around $b_i, \gamma_i = 1$, for each component in ρ or z coordinate one gets a separated equation and thus obtains four coupled equations. The dispersion relation for the frequency of the monopole and quadrupole modes can be determined by the condition for existence of nontrivial solutions, that is,

$$\det \left\| \omega^2 - \mathbf{A}_c \right\| = 0, \tag{14}$$

where the matrix

$$\mathbf{A}_c = \begin{bmatrix} (4 - B_{\rho\rho})\omega_{\perp b}^2 & (1 - B_{\rho z})\omega_{\perp b}^2 & B_{\rho\rho}\omega_{\perp b}^2 & B_{\rho z}\omega_{\perp b}^2 \\ (2 - B_{z\rho})\omega_{zb}^2 & (3 - B_{zz})\omega_{zb}^2 & B_{z\rho}\omega_{zb}^2 & B_{zz}\omega_{zb}^2 \\ D_{\rho\rho}\omega_{\perp f}^2 & D_{\rho z}\omega_{\perp f}^2 & (4 - D_{\rho\rho})\omega_{\perp f}^2 & -(F_\rho + D_{\rho z})\omega_{\perp f}^2 \\ D_{z\rho}\omega_{zf}^2 & D_{zz}\omega_{zf}^2 & -(2F_z + D_{z\rho})\omega_{zf}^2 & (4 + F_z - D_{zz})\omega_{zf}^2 \end{bmatrix}.$$

For each frequency of modes, the corresponding nontrivial solution, denoted by $(A_{b1}, A_{b2}, A_{f1}, A_{f2})$, gives the amplitude of the small density oscillations. As the system is composed of two kinds of particle, one would expect an emergence of two type of collective oscillations for each multipole. We thus define the mixing angle

$$\theta = \arcsin \left(\sqrt{\frac{A_{b1}^2 + A_{b2}^2}{A_{b1}^2 + A_{b2}^2 + A_{f1}^2 + A_{f2}^2}} \right), \quad (15)$$

to characterize the degree of mixing between bosonic and fermionic collective motions. As a limiting case, $\theta = \pi/2$ or 0 corresponds to the purely (decoupled) bosonic or fermionic oscillations, respectively.

In the special case of spherical traps, the monopole and quadrupole modes are decoupled. As shown in the Appendix, the dimensionless parameters $B_{\alpha\beta}$ (F_α , $D_{\alpha\beta}$) can further be reduced to a single value B (F , D),

$$\begin{aligned} B &= \frac{g_{bf}}{m_b\omega_b^2 N_b \langle r^2 \rangle_b} \int 4\pi r^2 dr \frac{dn_f^0(r)}{dr} r^2 \frac{dn_b^0(r)}{dr}, \\ F &= \frac{g_{bf}}{m_f\omega_f^2 N_f \langle r^2 \rangle_f} \int 4\pi r^2 dr \frac{dn_b^0(r)}{dr} r n_f^0(r), \\ D &= \frac{g_{bf}}{m_f\omega_f^2 N_f \langle r^2 \rangle_f} \int 4\pi r^2 dr \frac{dn_b^0(r)}{dr} r^2 \frac{dn_f^0(r)}{dr}. \end{aligned} \quad (16)$$

Accordingly, the dispersion relation (14) for the frequency of modes takes the following simple form,

$$\begin{aligned} \omega_M^2 &= \frac{1}{2} \left\{ [(5 - B)\omega_b^2 + (4 - F - D)\omega_f^2] \right. \\ &\quad \left. \pm \left([(5 - B)\omega_b^2 - (4 - F - D)\omega_f^2]^2 + 4BD\omega_b^2\omega_f^2 \right)^{1/2} \right\}, \end{aligned} \quad (17)$$

$$\begin{aligned} \omega_Q^2 &= \frac{1}{5} \left\{ [(5 - B)\omega_b^2 + (10 + 5F - D)\omega_f^2] \right. \\ &\quad \left. \pm \left([(5 - B)\omega_b^2 - (10 + 5F - D)\omega_f^2]^2 + 4BD\omega_b^2\omega_f^2 \right)^{1/2} \right\}, \end{aligned} \quad (18)$$

where the suffix M , Q denote monopole and quadrupole modes, respectively.

B. hydrodynamic regime

In the hydrodynamic regime, one assumes that local equilibrium has been established for the ground-state density profiles and it is maintained during dynamic fluctuations of the particle densities. A useful description of the dynamics of the Fermi gas in this regime is based on the Euler equation of motion [31,32],

$$\begin{aligned} \frac{\partial n_f}{\partial t} + \nabla \cdot (\mathbf{v}_f n_f) &= 0, \\ m_f \frac{\partial v_{fi}}{\partial t} + \frac{1}{n_f} \frac{\partial P(\mathbf{r}, t)}{\partial r_i} + m_f \sum_j v_{fj} \frac{\partial v_{fi}}{\partial r_j} + \frac{\partial}{\partial r_i} (V_{ho}^f + g_{bf} n_b) &= 0, \end{aligned} \quad (19)$$

where the pressure $P(\mathbf{r}, t) = \frac{2}{5} \frac{\hbar^2 (6\pi^2)^{2/3}}{2m_f} n_f^{5/3}(\mathbf{r}, t)$ in the local density approximation [32]. Without the boson-fermion interaction ($g_{bf} = 0$), Eq. (19) still admits a simple scaling solution [31,30], *i.e.*,

$$\begin{aligned} n_f(\mathbf{r}, t) &= \frac{1}{\prod_j \gamma_j(t)} n_f^0 \left(\frac{r_i}{\gamma_i(t)} \right), \\ v_{fi}(\mathbf{r}, t) &= \frac{1}{\gamma_i(t)} \frac{d\gamma_i(t)}{dt} r_i, \end{aligned} \quad (20)$$

which leads the following equations for the scaling parameters $\gamma_i(t)$:

$$\ddot{\gamma}_i(t) + \omega_{if}^2(t) \gamma_i(t) - \frac{\omega_{if}^2(0)}{\gamma_i(t) [\prod_j \gamma_j(t)]^{2/3}} = 0. \quad (21)$$

In the presence of a nonzero g_{bf} , one may still expect the validity of such scaling ansatz in the weakly coupled limit, although there is no verification by the other method (Note that the sum-rule approach is only applicable in the collisionless regime). Along the same line as in the previous subsection, after substituting the scaling ansatz (20) into equation (19) and taking the moment with respect to r_i^2 , one ultimately finds the differential equations satisfied by $\gamma_i(t)$,

$$\begin{aligned}
& \ddot{\gamma}_i(t) + \omega_{if}^2(t)\gamma_i(t) - \frac{\omega_{if}^2(0)}{\gamma_i(t) [\prod_j \gamma_j(t)]^{2/3}} \\
& + \frac{g_{bf}}{m_f N_f \langle R_i^2 \rangle_f} \frac{1}{\gamma_i \prod_j \gamma_j} \int d^3 \mathbf{R} \frac{\partial n_b^0(\mathbf{R})}{\partial R_i} R_i n_f^0\left(\frac{b_i}{\gamma_i} R_i\right) \\
& - \frac{g_{bf}}{m_f N_f \langle R_i^2 \rangle_f} \frac{1}{\gamma_i [\prod_j \gamma_j]^{2/3}} \int d^3 \mathbf{R} \frac{\partial n_b^0(\mathbf{R})}{\partial R_i} R_i n_f^0(\mathbf{R}) = 0,
\end{aligned} \tag{22}$$

which differ from Eqs. (10) for the collisionless regime.

Eqs. (9) and (22) can be linearized around the equilibrium state and combined to yield the determinant,

$$\det \left\| \omega^2 - \mathbf{A}_h \right\| = 0, \tag{23}$$

$$\mathbf{A}_h = \begin{bmatrix} (4 - B_{\rho\rho})\omega_{\perp b}^2 & (1 - B_{\rho z})\omega_{\perp b}^2 & B_{\rho\rho}\omega_{\perp b}^2 & B_{\rho z}\omega_{\perp b}^2 \\ (2 - B_{z\rho})\omega_{zb}^2 & (3 - B_{zz})\omega_{zb}^2 & B_{z\rho}\omega_{zb}^2 & B_{zz}\omega_{zb}^2 \\ D_{\rho\rho}\omega_{\perp f}^2 & D_{\rho z}\omega_{\perp f}^2 & \left(\frac{10}{3} - \frac{2F_\rho}{3} - D_{\rho\rho}\right)\omega_{\perp f}^2 & \left(\frac{2}{3} - \frac{F_\rho}{3} - D_{\rho z}\right)\omega_{\perp f}^2 \\ D_{z\rho}\omega_{zf}^2 & D_{zz}\omega_{zf}^2 & \left(\frac{4}{3} - \frac{2F_z}{3} - D_{z\rho}\right)\omega_{zf}^2 & \left(\frac{8}{3} - \frac{F_z}{3} - D_{zz}\right)\omega_{zf}^2 \end{bmatrix},$$

which gives rise to the dispersion relation in the hydrodynamic regime.

Finally, the frequency of the monopole and quadrupole modes for the spherical traps is obtained by rewriting $B_{\alpha\beta}$ (F_α , $D_{\alpha\beta}$) in terms of B (F , D),

$$\begin{aligned}
\omega_M^2 = & \frac{1}{2} \left\{ \left[(5 - B)\omega_b^2 + (4 - F - D)\omega_f^2 \right] \right. \\
& \left. \pm \left(\left[(5 - B)\omega_b^2 - (4 - F - D)\omega_f^2 \right]^2 + 4BD\omega_b^2\omega_f^2 \right)^{1/2} \right\},
\end{aligned} \tag{24}$$

$$\begin{aligned}
\omega_Q^2 = & \frac{1}{5} \left\{ \left[(5 - B)\omega_b^2 + (5 - D)\omega_f^2 \right] \right. \\
& \left. \pm \left(\left[(5 - B)\omega_b^2 - (5 - D)\omega_f^2 \right]^2 + 4BD\omega_b^2\omega_f^2 \right)^{1/2} \right\}.
\end{aligned} \tag{25}$$

Eqs. (17) and (24) explicitly show that the frequency of monopole oscillations coincides in the collisionless and hydrodynamic regime. This fact is a reminiscent of properties of a classical gas confined in an isotropic traps ($\omega_x = \omega_y = \omega_z = \omega_0$) [39,40], in which the monopole oscillation of frequency $\omega = 2\omega_0$ is an exact undamped solution of the full Boltzmann

equation. Analogously, in the boson-fermion mixtures the monopole excitation might also be undamped in all collisional regimes from the collisionless to the hydrodynamic one.

At the end of this section, we briefly mention the whole process of the numerical calculations that consists of three stages. First, one has to find the equilibrium ground-state densities at low temperature, which *approximately* satisfy the following coupled equations in the Thomas-Fermi approximation [10],

$$\begin{aligned} V_{ho}^b(\rho, z) + g_{bb}n_b^0(\rho, z) + g_{bf}n_f^0(\rho, z) &= \mu_b, \\ \frac{\hbar^2}{2m_f} \left(6\pi^2 n_f^0(\rho, z) \right)^{2/3} + V_{ho}^f(\rho, z) + g_{bf}n_b^0(\rho, z) &= \mu_f, \end{aligned} \quad (26)$$

where $\mu_{b,f}$ is the chemical potential. Then one computes the dimensionless parameters $B_{\alpha\beta}$, F_α , and $D_{\alpha\beta}$ ($\alpha, \beta = \rho$ or z), and finally, one solves the Eqs. (14) and (23) (in the case of spherical traps, one explicitly uses Eqs. (17), (18) and (25)) to obtain the frequency of the monopole and quadrupole modes. The mixing angle for each mode is also simultaneously calculated.

III. RESULT

In this work, we have performed a numerical calculation for $N_b = N_f = 10^6$, where the number of bosons and fermions is large enough to ensure the validity of the Thomas-Fermi approximation, *i.e.*, $N_b a_{bb}/a_\perp^b \gg 1$ and $N_f \gg 1$ [10,14]. We take the harmonic oscillator length $a_\perp^b = \sqrt{\frac{\hbar}{m_b \omega_{\perp b}}}$ and $\hbar \omega_{\perp b}$ as units, and define the scaled dimensionless variables: the coordinates $\tilde{\rho} = \rho/a_\perp^b$, $\tilde{z} = z/a_\perp^b$, boson/fermion densities $\tilde{n}_{b,f}^0 = n_{b,f}^0 (a_\perp^b)^3$, interactions strength $\tilde{g}_{bb} = g_{bb} / \left[\hbar \omega_{\perp b} (a_\perp^b)^3 \right] = 4\pi a_{bb}/a_\perp^b$, and chemical potentials $\tilde{\mu}_{b,f} = \mu_{b,f} / (\hbar \omega_{\perp b})$. We also introduce the quantities $\alpha = m_f/m_b$, $\beta = \omega_{\perp f}/\omega_{\perp b}$, $\lambda = \omega_{zb}/\omega_{\perp b} = \omega_{zf}/\omega_{\perp f}$, and $\kappa = g_{bf}/g_{bb}$ to parameterize the different mass of the two components, anisotropy of traps, and boson-fermion coupling relative to the boson-boson interaction. The constraint $\alpha\beta^2 = 1$ is always satisfied since in experiments both bosons and fermions experience the same trapping potential. In the scaled units, the coupled Thomas-Fermi equations (26) take the form,

$$\begin{aligned} \frac{1}{2} \left(\tilde{\rho}^2 + \lambda^2 \tilde{z}^2 \right) + \tilde{g}_{bb} n_b^0 + \kappa \tilde{g}_{bb} n_f^0 &= \tilde{\mu}_b, \\ \frac{1}{2\alpha} \left(6\pi^2 n_f^0 \right)^{2/3} + \frac{1}{2} \left(\tilde{\rho}^2 + \lambda^2 \tilde{z}^2 \right) + \kappa \tilde{g}_{bb} n_b^0 &= \tilde{\mu}_f. \end{aligned} \quad (27)$$

It is convenient to obtain the solutions to Eq. (27) by iterative insertion of one density distribution in the other equation and numerically searching for the chemical potential $\tilde{\mu}_b$ and $\tilde{\mu}_f$ yielding the desired number of particles.

We shall investigate the behavior of monopole and quadrupole modes against boson-fermion coupling κ for three typical values of \tilde{g}_{bb} . First of all, we consider the relevant parameters for a boson-fermion mixture composed of ^{40}K (fermion) and ^{87}Rb (boson), which has been recently realized by the LENS group [9]. In order to emphasize the interplay of collective modes of bosons and fermions due to the nonzero g_{bf} (the degree of mixing will be maximum if their bare mode frequencies are close to each other), we will consider the same mass ($m_b = m_f = m$) and trapping frequency ($\omega_b = \omega_f = \omega_0$) for bosons and fermions in most cases, although the realistic mass of ^{87}Rb is about two times larger than that of ^{40}K . As in the experiment, we take the radial harmonic frequency of $\omega_{\perp b} = 2\pi \times 216 \text{ s}^{-1}$ for ^{87}Rb and the boson-boson s -wave scattering length of $a_{bb} = 110a_0 = 5.9 \text{ nm}$, which gives the rescaled interaction strength $\tilde{g}_{bb} = 0.1$. In the ground state the fermions have a much broader distribution than bosons because of the Pauli principle and the bosons are completely immersed in the Fermi sea [9]. Secondly, as an opposite limit, we consider the case in which the fermions and boson have approximately the same radius and significantly overlap with each other. Within the Thomas-Fermi approximation, at $\kappa = 0$, the radius of the Bose condensate and zero-temperature Fermi gas in the scaled units are given by $r_b = (15N_b\tilde{g}_{bb}/4\pi)^{1/5}$ and $r_f = (48N_f)^{1/6}$, respectively. Equating these two numbers we get the constraint: $\tilde{g}_{bb} = 2.11$. Finally, we take $\tilde{g}_{bb} = 0.5$ for the intermediate regime. It should be noted that in experiments the interaction strength \tilde{g}_{bb} can be controlled by using Feshbach resonances [41].

In the section IIIA, we briefly estimate the criterion for establishing the hydrodynamic regime. In the next sections IIIB and IIIC, we analyze the collective modes in the collisionless

and hydrodynamic regime for a spherical trap. The results for a cylindrically symmetric trap will be presented in section IIID.

A. the criterion to establish the hydrodynamic regime

A hydrodynamic regime is established in the low temperature alkali vapor when the inequality

$$\omega\tau \ll 1 \quad (28)$$

holds, where τ being the collision time for incoherent scattering of fermions against the condensate and ω being on the scale of the trap frequency ($\omega \simeq \omega_f$) for the low-lying modes. At low temperature, the dominate collision procedure comes from the scattering between a fermion and a condensate boson, which generates another fermion and a Bogoliubov quasi-particle. In this procedure, the mean velocity of the condensate boson is negligible relative to that of the fermions. A naive estimate for the collision time can thus be written as

$$\tau^{-1} \approx n_b (4\pi a_{bf}^2) v_F \left(\frac{T}{T_F}\right)^2, \quad (29)$$

where $n_b (4\pi a_{bf}^2) v_F$ is the classical collisional frequency and the factor $\left(\frac{T}{T_F}\right)^2$ results from the Pauli blocking. By setting $n_b = N_b/(4\pi r_b^3/3)$ and taking $v_F = \sqrt{2\mu_F/m_f}$ for a spherical trap, we approximately have

$$\frac{1}{\omega_f \tau} \approx 3 \times 2^{1/2} \times 6^{1/6} \times \left(\frac{4\pi}{15\tilde{g}_{bb}}\right)^{3/5} N_b^{2/5} N_f^{1/6} \tilde{a}_{bf}^2 \left(\frac{T}{T_F}\right)^2, \quad (30)$$

where $\tilde{a}_{bf} = a_{bf}/a_{ho}$ is the s-wave boson-fermion scattering length in the scaled units.

For illustrative purposes we again consider the boson-fermion mixture of ^{40}K and ^{87}Rb studied by the LENS group. From the known values of the ^{40}K - ^{87}Rb scattering length $a_{bf} = 300a_0$, and $\tilde{g}_{bb} = 0.1$, we have

$$\frac{1}{\omega_f \tau} \approx 29 \times \left(\frac{T}{T_F}\right)^2, \quad (31)$$

for $N_b = N_f = 10^6$. As anticipated earlier in the introduction, the temperature of order $T \sim 0.5T_F$ would suffice to verify the inequality (28) with $\omega \simeq \omega_f$, and therefore to reach the hydrodynamic regime.

In the next subsections, we shall consider the behavior of the collective modes against the boson-fermion interaction strength, rather than the temperature. It should be reminded that for a fixed temperature, our results for the hydrodynamic regime (or the collisionless regime) are only valid at $|g_{bf}| \gg g_{bf}^c$ (or $|g_{bf}| \ll g_{bf}^c$), where g_{bf}^c can be roughly determined from Eq. (30).

B. collisionless modes in a spherical trap

Figures 1 and 2, respectively, show the frequencies and mixing angles of the monopole and quadrupole modes as a function of κ for the case in which the bosons and fermions have the same mass ($m_b = m_f = m$) and trapping frequency ($\omega_b = \omega_f = \omega_0$). As we have anticipated in the last section, there are two types of collective oscillations for each multipole. For clarity, we plot the lower and higher frequency modes by the solid and dashed lines, respectively.

The collisionless collective modes for the weak boson-boson interaction has been investigated earlier by a sum-rule approach in Ref. [24]. As shown in the figures 1a and 2a, the result for $\tilde{g}_{bb} = 0.1$ agrees well with that obtained by the sum-rule approach in the whole regime of κ if we use the same parameters (see, for example, the figures 2a and 2b in Ref. [24]). This excellent agreement in some sense justifies our assumption of the scaling form of solutions to Eqs. (1) and (2). We believe the same is true in the hydrodynamic regime.

The most remarkable feature in figures 1 and 2 is the existence of a specific value $\kappa_c \neq 0$, at which the collective oscillation of each mode becomes purely bosonic or fermionic. κ_c coincides with the critical values of phase separation for the strong boson-boson interaction and becomes unity for the weak or medium boson-boson interaction. The existence of κ_c can be readily understood from the distribution of boson and fermion densities. As shown

by Mølmer [10], for a positive boson-fermion interaction, the fermions are squeezed out the center. As κ increases, they will eventually form a shell-like distribution around the surface of bosons for $\kappa \geq 1$ and will be completely pushed away from the center at a critical value where the phase separation occurs. For the weak or medium boson-boson interaction, as shown in the figure 3a, precisely at $\kappa = 1$ the fermions experience a constant potential in the region occupied by bosons and therefore uniformly distributed there. As a result, the parameters B and D defined in Eqs. (16) will vanish and consequently the bosonic and fermion part in the determinant (14) will be completely decoupled. Therefore the collective oscillation of modes will be purely bosonic or fermionic. Analogous mechanics works for the case of strong boson-boson interaction, where B and D will be zero at the critical value of phase separation that is smaller than unity. Note, however, that in this case our assumption of the scaling ansatz will apparently break down once $\kappa > \kappa_c$, and the phase separation will lead to a decoupling of the collective modes.

An immediate application of the above observation is that we can derive an analytic expression for the frequency of each mode in the weak or moderately strong boson-boson interaction in which $\kappa_c = 1$. As illustrated in figure 3b, for small values of κ , the B , F , and D can be well approximated by $b_0\kappa(1 - \kappa)$, $f_0\kappa$, and $d_0\kappa(1 - \kappa)$, respectively, where $b_0 = (dB/d\kappa)_{\kappa=0}$, $f_0 = (dF/d\kappa)_{\kappa=0}$, and $d_0 = (dD/d\kappa)_{\kappa=0}$. The form of B and D follows the fact that they have to vanish at both $\kappa = 0$ and $\kappa = 1$. In the Thomas-Fermi approximation, one may obtain,

$$\begin{aligned} b_0 &= +\frac{224}{\pi} \left(\frac{N_f}{N_b}\right) x^5 \int_0^1 y^6 (1 - x^2 y^2)^{1/2} dy, \\ f_0 &= -\frac{256}{3\pi} x^5 \int_0^1 y^4 (1 - x^2 y^2)^{3/2} dy, \\ d_0 &= +\frac{256}{\pi} x^7 \int_0^1 y^6 (1 - x^2 y^2)^{1/2} dy, \end{aligned} \quad (32)$$

where $x = \frac{r_b}{r_f} = \left(\frac{m_f \omega_f}{m_b \omega_b}\right)^{1/2} (15N_b \tilde{g}_{bb}/4\pi)^{1/5} / (48N_f)^{1/6} \leq 1$ is the ratio of the radius of the Bose condensate and zero-temperature Fermi gas. The frequencies obtained by combining

Eqs. (17), (18) and (32) are plotted in figures 1 and 2 by thin lines. We find that it is in a good agreement with the full numerical calculations for a wide regime of κ .

Below we discuss the behavior of the frequencies ω_α of each mode by defining three regions of κ : (I) $\kappa < 0$, (II) $0 \leq \kappa < \kappa_c$, and (III) $\kappa_c \leq \kappa$.

(a) *Monopole*. For a noninteracting boson-fermion system the low-lying monopole mode is the fermionic oscillation with frequency $\omega_M^L = 2\omega_0$, while the higher mode is the bosonic one with $\omega_M^H = \sqrt{5}\omega_0$ in the Thomas-Fermi approximation. Around $\kappa = 0$, one may obtain $\omega_M^L \approx 2\omega_0 \left(1 - \frac{d_0+f_0}{8}\kappa\right)$ and $\omega_M^H \approx \sqrt{5}\omega_0 \left(1 - \frac{b_0}{10}\kappa\right)$. The essential features of the monopole mode as a function of κ can be summarized as follows. (i) The curve for the high-lying bosonic mode seems like a parabola. Indeed, the frequency for the bosonic mode is always found to be degenerate at $\kappa = 0$ and $\kappa = \kappa_c$. In region II, the frequency varies slowly against κ and is slightly smaller than the value of $\sqrt{5}\omega_0$ in the noninteracting limit. Here, the boson density distribution expands slightly compared with that of the noninteracting boson-fermion system due to the weakly repulsive boson-fermion interaction and simultaneously the bosons experience a weaker effective confinement. In the region I and III, the situation is quite different: the bosons are heavily compressed by either the attractive or strong repulsive boson-fermion interaction. This strong confinement leads to a steep rise of frequency with increasing $|\kappa|$. (ii) The behavior of the frequency for low-lying fermionic mode against κ is more complicated. As the boson-boson interaction strength \tilde{g}_{bb} increases, the sign of the derivative of the curve at $\kappa = 0$ changes from positive to negative. At $\tilde{g}_{bb} = 2.11$ a large dip appears in the region II. On the other hand, at a large negative values of κ , as pointed out by Miyakawa *et al.* [24], we find a sharp decrease of the frequency towards the instability point of the ground state. (iii) Finally, at large values of $|\kappa|$ the mixing angle for both the low-lying and high-lying modes becomes close to $\pi/4$, suggesting that the bosons and fermions are highly correlated in the collective oscillations. The degree of mixing is enhanced as one increases \tilde{g}_{bb} .

(b) *Quadrupole*. For the quadrupole excitation (figure 2), the lower and higher energy mode becomes bosonic and fermionic oscillation, respectively. To the first order of κ the

frequencies of the lower and the higher quadrupole modes are given by $\omega_Q^L \approx \sqrt{2}\omega_0 \left(1 - \frac{b_0}{10}\kappa\right)$ and $\omega_Q^H \approx 2\omega_0 \left(1 + \frac{5f_0-d_0}{20}\kappa\right)$. For those modes, similar mechanisms as for the monopole mode are still at work concerning the dependence on κ . However, the role of the boson-fermion interaction is much reduced compared with the monopole case as seen by the factor $1/5$ in Eq. (18), which reflects that the quadrupole oscillation has 5 different components [24]. In addition, the behavior of the high-lying fermionic mode is somewhat simpler. The frequency is always decreases around $\kappa = 0$ as κ increases.

C. hydrodynamic modes in a spherical trap

In section II, we have analytically showed that in a spherical trap the frequency of monopole oscillations coincides in the collisionless and hydrodynamic regime. Here we find a dramatic difference for the quadrupole mode. In the figure 4, we plot the frequencies and mixing angles of the quadrupole modes in the hydrodynamic regime against κ . The parameters are the same as that in figures 1 and 2. Compared with the result for the quadrupole mode in the collisionless regime (figure 2), an interesting feature emerges: The frequency of the low-lying mode (high-lying mode) is always fixed to $\sqrt{2}\omega_0$ in the region I and III (region II), independently of the value of κ , and the corresponding mixing angle is exactly $\pi/4$ even around $\kappa = 0$. This strongly suggests that in this case the collective oscillation with equal bosonic and fermionic amplitudes generates an exact eigenstate of the system, regardless of the boson-fermion interaction. It resembles the Kohn mode in the isotropic harmonic traps. Indeed, the behavior of the frequencies shown in figure 4 is quite similar to that of a dipole mode in the collisionless limit (see, for example, the figure 2c in Ref [24]). The above feature can also be explained explicitly from Eq. (25). For the case considered here, $\omega_b = \omega_f = \omega_0$, we have $\omega_Q = \sqrt{2}\omega_0 \{1 - [(B + D) \pm |B + D|]/10\}^{1/2}$, and thus one branch of ω_Q will always be $\sqrt{2}\omega_0$.

The strong mixing of the bosonic and fermionic oscillation stated above in fact arises from the “on resonance” condition, that is, the frequency of the bosonic and fermionic quadrupole

modes in hydrodynamic regime is degenerate in the noninteracting limit of $\kappa = 0$. As shown in figure 5, once one moves away from the “on resonance” condition by changing m_f/m_b , the degree of mixing will be much reduced.

D. a cylindrically symmetric trap

In this subsection, we consider a cylindrical trap that is more relevant to the experiment. Figures 6 and 7, respectively, display the frequencies of each mode for a cigar-shaped ($\lambda = 0.5$) and disk-shaped ($\lambda = 2.0$) trap in the collisionless (thick lines) and hydrodynamic (thin lines) regime. As the monopole and quadrupole modes are coupled away from $\lambda = 1$, we denote the two higher and two lower modes as quasi-monopole and quasi-quadrupole ones, respectively. In the literature, the former one is also called as transverse breathing mode in the limit of $\lambda \rightarrow 0$. As one may expect, in the cylindrical trap the frequency of quasi-monopole mode in the collisionless and hydrodynamic regime is no longer degenerate.

(a) *a cigar-shaped trap.* For the quasi-monopole excitation (figure 6a), the lower and higher energy mode in both regimes are fermionic and bosonic oscillations. In region I and III, the frequencies for the high-lying mode in the collisionless and hydrodynamic regime are almost the same and they only differ slightly in region II. In contrast, for the low-lying mode the frequencies in two regimes have significant differences. In particular, as κ decreases towards the instability point of the ground state, the frequency in the collisionless regime rises up steeply, while the one in the hydrodynamic regime shows a sharp decrease. For the quasi-quadrupole excitation (figure 6b), on the other hand, the frequencies for each mode bears a lot of similarity as that in the spherical case. We thus don’t discuss them further.

(b) *a disk-shaped trap.* In this case (figure 7), the lower and higher energy mode for both quasi-monopole and quasi-quadrupole excitations in the collisionless regime are bosonic and fermionic oscillations, respectively. The opposite is true in the hydrodynamic regime. Most interestingly, the soften of the mode frequency towards the instability point of the ground state now appears in the low-lying mode for the quasi-quadrupole excitations, rather than

the monopole one.

IV. SUMMARY AND DISCUSSION

Ultracold boson-fermion mixtures of alkali atoms have recently been the subject of intensive experimental research. As an important tool to characterize the behaviour of this kind of many-body system, the investigation of collective oscillations will be of particular interest. In this paper, with the help of Thomas-Fermi approximation and a scaling solution we have studied the behavior of monopole and quadrupole excitations against the boson-fermion interaction in two limiting cases: the collisionless and hydrodynamic regime. For a spherical trap, the frequency of monopole mode is identical in both regimes, analogous to that of a classical gas, which is undamped in all collisional regimes. In contrast, the frequency of quadrupole mode differs largely in these two limits. Most interestingly, in the case of same trapping frequency for the two components ($\omega_b = \omega_f$) and hydrodynamic regime, the quadrupole oscillations with equal bosonic and fermionic amplitudes are found to generate an exact eigenstate of the system, regardless of the boson-fermion interaction. It indeed resembles the Kohn mode for the dipole excitation.

While we have restricted the discussion to the collisionless and hydrodynamic regime, it should be explicitly remarked from the experimental point of view that it is more interesting to investigate the *crossover* between these two limits [42], which might be realized in the experiment by changing the temperature or controlling the particle-particle interaction through Feshbach resonances. In theory, such crossover might be investigated by adding a collision term (I_{coll}) to Eq. (2).

We are aware of that the above results are based on the assumption of the simple scaling solution. Its validity has been partly justified by the good agreement between our results and that obtained by a sum-rule approach. However, in case of large boson-fermion interaction, the spectrum of lowest collective excitations might be fragmented [25,26,43]. As a result, both the sum-rule approach and the approximation of simple scaling solution will break

down. In those regions, a refined treatment is deserved.

V. ACKNOWLEDGEMENTS

We acknowledge stimulating discussions with G. Modugno, M. Modugno, F. Ferlaino, and M. Inguscio. One of us (X.-J. Liu) wishes to thank the Abdus Salam International Centre for Theoretical Physics (ICTP) for their hospitality during the early stages of this work. X.-J. Liu is supported by the CAS K.C.Wang Post-doctoral Research Award Fund, the Chinese Post-doctoral Fund and the NSF-China.

VI. APPENDIX

This appendix is devoted to simplify the expressions of B_{ik} , F_i , and D_{ik} in case of cylindrical symmetric or spherical traps. For a cylindrical trap, the boson and fermion density distribution depend on $\rho = (R_x^2 + R_y^2)^{1/2}$, $z = R_z$ only. By writing

$$\begin{aligned}\frac{\partial}{\partial R_x} &= \frac{R_x}{\rho} \frac{\partial}{\partial \rho} = \cos \phi \frac{\partial}{\partial \rho}, \\ \frac{\partial}{\partial R_y} &= \frac{R_y}{\rho} \frac{\partial}{\partial \rho} = \sin \phi \frac{\partial}{\partial \rho}, \\ \frac{\partial}{\partial R_z} &= \frac{\partial}{\partial z},\end{aligned}\tag{A1}$$

one has

$$\begin{aligned}B_{xx} &= \frac{g_{bf}}{m_b \omega_{\perp b}^2(0) N_b \langle R_x^2 \rangle_b} \int d^3 \mathbf{R} \frac{\partial n_f^0(\mathbf{R})}{\partial R_x} R_x R_x \frac{\partial n_b^0(\mathbf{R})}{\partial R_x}, \\ &= \frac{\int_0^{2\pi} d\phi \cos^4 \phi}{\int_0^{2\pi} d\phi \cos^2 \phi} \left[\frac{g_{bf}}{m_b \omega_{\perp b}^2(0) N_b \langle \rho^2 \rangle_b} \int \rho d\rho dz \frac{\partial n_f^0}{\partial \rho} \rho^2 \frac{\partial n_b^0}{\partial \rho} \right] \\ &= \frac{3}{4} B_{\rho\rho},\end{aligned}$$

where

$$B_{\rho\rho} = \frac{g_{bf}}{m_b \omega_{\perp b}^2(0) N_b \langle \rho^2 \rangle_b} \int \rho d\rho dz \frac{\partial n_f^0}{\partial \rho} \rho^2 \frac{\partial n_b^0}{\partial \rho}.$$

Similarly, one finds the relations:

$$\begin{aligned}
B_{xx} &= 3B_{\rho\rho}/4, & B_{xy} &= B_{\rho\rho}/4, & B_{xz} &= B_{\rho z}, \\
B_{yx} &= B_{\rho\rho}/4, & B_{yy} &= 3B_{\rho\rho}/4, & B_{yz} &= B_{\rho z}, \\
B_{zx} &= B_{z\rho}/2, & B_{zy} &= B_{z\rho}/2, & B_{zz} &= B_{zz}, \\
F_x &= F_\rho, & F_y &= F_\rho, & F_z &= F_z,
\end{aligned} \tag{A2}$$

$$\begin{aligned}
D_{xx} &= 3D_{\rho\rho}/4, & D_{xy} &= D_{\rho\rho}/4, & D_{xz} &= D_{\rho z}, \\
D_{yx} &= B_{\rho\rho}/4, & D_{yy} &= 3B_{\rho\rho}/4, & D_{yz} &= D_{\rho z}, \\
D_{zx} &= D_{z\rho}/2, & D_{zy} &= D_{z\rho}/2, & D_{zz} &= D_{zz},
\end{aligned}$$

where $B_{\alpha\beta}$, F_α , and $D_{\alpha\beta}$ ($\alpha, \beta = \rho$ or z) take the form,

$$\begin{aligned}
B_{\rho\rho} &= \frac{g_{bf}}{m_b\omega_{\perp b}^2(0)N_b\langle\rho^2\rangle_b} \int \rho d\rho dz \frac{\partial n_f^0}{\partial\rho} \rho^2 \frac{\partial n_b^0}{\partial\rho}, \\
B_{\rho z} &= \frac{g_{bf}}{m_b\omega_{\perp b}^2(0)N_b\langle\rho^2\rangle_b} \int \rho d\rho dz \frac{\partial n_f^0}{\partial\rho} \rho z \frac{\partial n_b^0}{\partial z}, \\
B_{z\rho} &= \frac{g_{bf}}{m_b\omega_{zb}^2(0)N_b\langle z^2\rangle_b} \int \rho d\rho dz \frac{\partial n_f^0}{\partial z} z \rho \frac{\partial n_b^0}{\partial\rho}, \\
B_{zz} &= \frac{g_{bf}}{m_b\omega_{zb}^2(0)N_b\langle z^2\rangle_b} \int \rho d\rho dz \frac{\partial n_f^0}{\partial z} z^2 \frac{\partial n_b^0}{\partial z}, \\
F_\rho &= \frac{g_{bf}}{m_f\omega_{\perp f}^2(0)N_f\langle\rho^2\rangle_f} \int \rho d\rho dz \frac{\partial n_b^0}{\partial\rho} \rho n_f^0, \\
F_z &= \frac{g_{bf}}{m_f\omega_{zf}^2(0)N_f\langle z^2\rangle_f} \int \rho d\rho dz \frac{\partial n_b^0}{\partial z} z n_f^0, \\
D_{\rho\rho} &= \frac{g_{bf}}{m_f\omega_{\perp f}^2(0)N_f\langle\rho^2\rangle_f} \int \rho d\rho dz \frac{\partial n_b^0}{\partial\rho} \rho^2 \frac{\partial n_f^0}{\partial\rho}, \\
D_{\rho z} &= \frac{g_{bf}}{m_f\omega_{\perp f}^2(0)N_f\langle\rho^2\rangle_f} \int \rho d\rho dz \frac{\partial n_b^0}{\partial\rho} \rho z \frac{\partial n_f^0}{\partial z}, \\
D_{z\rho} &= \frac{g_{bf}}{m_f\omega_{zf}^2(0)N_f\langle z^2\rangle_f} \int \rho d\rho dz \frac{\partial n_b^0}{\partial z} z \rho \frac{\partial n_f^0}{\partial\rho}, \\
D_{zz} &= \frac{g_{bf}}{m_f\omega_{zf}^2(0)N_f\langle z^2\rangle_f} \int \rho d\rho dz \frac{\partial n_b^0}{\partial z} z^2 \frac{\partial n_f^0}{\partial z}.
\end{aligned} \tag{A3}$$

For a spherical trap, the density distribution is a function of $r = (\rho^2 + z^2)^{1/2}$ only. We thus define $\rho = r \sin \theta$ and $z = r \cos \theta$, where $\theta \in [0, \pi]$. After some straightforward algebra one finds,

$$B_{\rho\rho} = \frac{4}{5}B, \quad B_{\rho z} = \frac{1}{5}B, \quad B_{z\rho} = \frac{2}{5}B, \quad B_{zz} = \frac{3}{5}B,$$

$$F_\rho = F, \quad F_z = F, \tag{A4}$$

$$D_{\rho\rho} = \frac{4}{5}D, \quad D_{\rho z} = \frac{1}{5}D, \quad D_{z\rho} = \frac{2}{5}D, \quad D_{zz} = \frac{3}{5}D,$$

where B , F and D are given by Eqs. (16).

REFERENCES

- [1] M. H. Anderson, J. R. Ensher, M. R. Matthews, C. E. Wieman, and E. A. Cornell, *Science* **269**, 198 (1995).
- [2] K. B. Davis, M.-O. Mewes, M. R. Andrews, N. J. van Druten, d. S. Durfee, D. M. Kurn, and W. Ketterle, *Phys. Rev. Lett.* **75**, 3969 (1995).
- [3] F. Dalfovo, S. Giorgini, L. P. Pitaevskii, and S. Stringari, *Rev. Mod. Phys.* **71**, 463 (1999).
- [4] F. Chevy, V. Bretin, P. Rosenbusch, K. W. Madison, and J. Dalibard, *Phys. Rev. Lett.* **88**, 250402 (2002).
- [5] D. S. Jin, M. R. Matthews, J. R. Ensher, C. E. Wieman, and E. A. Cornell, *Phys. Rev. Lett.* **78**, 764 (1997); R. Onofrio, D. S. Durfee, C. Raman, M. Kohl, C. E. Kuklewicz, and W. Ketterle, *Phys. Rev. Lett.* **84**, 810 (2000).
- [6] O. M. Maragò, S. A. Hopkins, J. Alt, E. Hodby, G. Hechenblaikner, and C. J. Foot, *Phys. Rev. Lett.* **84**, 2056 (2000); O. M. Maragò, G. Hechenblaikner, E. Hodby, and C. J. Foot, *Phys. Rev. Lett.* **86**, 3938 (2001).
- [7] B. Demarco and D. S. Jin, *Science* **285**, 1703 (1999); B. Demarco, S. B. Papp, and D. S. Jin, *Phys. Rev. Lett.* **86**, 5409 (2001); S. R. Granade, M. E. Gehm, K. M. O'Hara, and J. E. Thomas, *Phys. Rev. Lett.* **88**, 120405 (2002).
- [8] A. G. Truscott, K. E. Strecker, W. I. McAlexander, G. B. Partridge, and R. G. Hulet, *Science* **291**, 2570 (2001); F. Schreck, L. Khaykovich, K. L. Corwin, G. Ferrari, T. Bourdel, J. Cubizolles, and C. Salomon, *Phys. Rev. Lett.* **87**, 080403 (2001); Z. Hadzibabic, C. A. Stan, K. Dieckmann, S. Gupta, M. W. Zwierlein, A. Gorlitz, and W. Ketterle, *Phys. Rev. Lett.* **88**, 160401 (2002).
- [9] G. Roati, F. Riboli, G. Modugno, and M. Inguscio, *Phys. Rev. Lett.* **89**, 150403 (2002).
- [10] K. Mølmer, *Phys. Rev. Lett.* **80**, 1804 (1998).

- [11] M. Amoruso, A. Minguzzi, S. Stringari, M. P. Tosi, and L. Vichi, Eur. Phys. J. D **4**, 261(1998).
- [12] M. J. Bijlsma, B. A. Heringa, and H. T. C. Stoof, Phys. Rev. A **61**, 053601 (2000).
- [13] L. Vichi, M. Inguscio, S. Stringari, and G. M. Tino, J. Phys. B **31**, L899 (1998); Eur. Phys. J. D **11**, 335 (2000).
- [14] N. Nygaard and K. Mølmer, Phys. Rev. A **59**, 2974 (1999).
- [15] X. X. Yi and C. P. Sun, Phys. Rev. A **64**, 043608 (2001).
- [16] L. Viverit, C. J. Pethick, and H. Smith, Phys. Rev. A **61**, 053605 (2000).
- [17] R. Roth and H. Feldmeier, Phys. Rev. A **65**, 021603(R) (2002).
- [18] T. Miyakawa, T. Suzuki, and H. Yabu, Phys. Rev. A **64**, 033611 (2001).
- [19] S. K. Yip, Phys. Rev. A **64**, 023609 (2001).
- [20] B. H. Valtan, M. Nishida, and S. Kurihara, Laser Physics **12**, 217 (2002).
- [21] H. Pu, W. Zhang, M. Wilkens, and P. Meystre, Phys. Rev. Lett. **88**, 070408 (2002).
- [22] C. P. Search, H. Pu, W. Zhang, and P. Meystre, Phys. Rev. A **65**, 063615 (2002).
- [23] A. Minguzzi and M. P. Tosi, Phys. Lett. A **268**, 142 (2000).
- [24] T. Miyakawa, T. Suzuki, and H. Yabu, Phys. Rev. A **62**, 063613 (2000).
- [25] P. Capuzzi and E. S. Hernández, Phys. Rev. A **64**, 043607 (2001).
- [26] T. Sogo, T. Miyakawa, T. Suzuki, and H. Yabu, Phys. Rev. A **66**, 013618 (2002).
- [27] G. Modugno, G. Roati, F. Riboli, F. Ferlaino, R. J. Brecha, and M. Inguscio, Science **297**, 2240 (2002).
- [28] Of course, in the case of cylindrical traps, the anisotropy introduces a coupling between the monopole and quadrupole modes, which are described by the quantum numbers ($n = 1$,

$l = 0, m = 0$) and $(n = 0, l = 2, m = 0)$, respectively.

- [29] D. Guéry-Odelin, Phys. Rev. A **66**, 033613 (2002).
- [30] C. Menotti, P. Pedri and S. Stringari, Phys. Rev. Lett. **89**, 250402 (2002).
- [31] Yu. Kagan, E. L. Surkov, and G. V. Shlyapnikov, Phys. Rev. A **55**, R18 (1997).
- [32] M. Amoruso, I. Meccoli, A. Minguzzi, and M. P. Tosi, Eur. Phys. J. D **7**, 441 (1999).
- [33] S. Stringari, Phys. Rev. Lett. **77**, 2360 (1996).
- [34] At low temperature, the collision term is mainly determined by the collisions between one fermion and one condensated boson, which scatters the fermion into another state and produce a Bogoliubov quasiparticle. For such collision procedure, one may derive the semi-classical equation of motions for the Wigner operator of either fermions or Bogoliubov quasiparticles, and one may find that the contribution of the collisions to the condensate is much smaller than that to the fermions.
- [35] D. A. Butts and D. S. Rokhsar, Phys. Rev. A **55**, 4346 (1997).
- [36] Y. Castin and R. Dum, Phys. Rev. Lett. **77**, 5315 (1996).
- [37] G. M. Bruun and C. W. Clark, Phys. Rev. A **61**, 061601 (2000).
- [38] In this case, the average is done by multiplying the equations by R_i and V_i and integrating over the phase space. See Ref. [29] for details.
- [39] L. Boltzmann, in *Wissenschaftliche Abhandlungen*, edited by F. Hasenorl (J. A. Barth, Leipzig, 1909), Vol. II, p. 83.
- [40] D. Guéry-Odelin, F. Zambelli, J. Dalibard, and S. Stringari, Phys. Rev. A **60**, 4851 (1999).
- [41] E. Tiesinga, A. J. Moerdijk, B. J. Verhaar, and H. T. C. Stoof, Phys. Rev. A **46** R1167 (1992); E. A. Donley *et al.*, Nature **412**, 295 (2001).
- [42] S. D. Gensemer and D. S. Jin, Phys. Rev. Lett. **87**, 173201 (2001).

[43] G. M. Bruun, Phys. Rev. A **63**, 043408 (2001).

Figures Captions

Fig. 1. The frequencies (upper part) and mixing angles (lower part) of the monopole mode in the collisionless regime as a function of the boson-fermion interaction, for a spherical trap with (a) $\tilde{g}_{bb} = 0.1$, (b) 0.5 and (c) 2.11. The other parameters are $N_b = N_f = 10^6$, $m_b = m_f = m$ (or $\omega_b = \omega_f = \omega_0$). The low-lying and high-lying frequency mode are denoted by the thick solid and dashed lines, respectively. The analytic solutions obtained by combining Eqs. (17), (18) and (32) are also plotted in figures (a) and (b) by thin lines. Note that in figure (c), the result is not meaningful at $\kappa > \kappa_c \approx 0.69$, where the phase separation will occur.

Fig. 2. The same as in fig. 1, but for the quadrupole mode.

Fig. 3. (a) The boson (solid line) and fermion (dashed line) density distribution for a spherical trap with $\tilde{g}_{bb} = 0.5$ and $\kappa = 1$. In this case, the fermions experience a constant potential in the region occupied by bosons and therefore uniformly distributed there. (b) $b = B/\kappa$, $f = F/\kappa$, and $d = D/\kappa$ as a function the boson-fermion interaction for a spherical trap with $\tilde{g}_{bb} = 0.5$. Note that precisely at $\kappa = 1$, $B = D = 0$.

Fig. 4. The same as in fig.1, but for the quadrupole mode in the hydrodynamic regime.

Fig. 5. The frequencies (upper part) and mixing angles (lower part) of the quadrupole mode in the hydrodynamic regime against the boson-fermion interaction, for a spherical trap with (a) $m_f/m_b = 0.8$ and (b) $m_f/m_b = 1.03$ at $\tilde{g}_{bb} = 0.5$. Since the boson and fermion trapping frequency is not the same, the mode frequency for bosons and fermions is no longer degenerate at $\kappa = 0$, *i.e.*, it is out of the resonance. As a result, the degree of mixing between bosonic and fermion collective oscillations is much reduced.

Fig. 6. The frequencies of each mode as a function of κ for a cigar-shaped trap with $\lambda = 0.5$. (a) quasi-monopole and (b) quasi-quadrupole. The results in the collisionless and hydrodynamic regime, respectively, are displayed by the thick and thin lines. The other parameters are $N_b = N_f = 10^6$, $m_b = m_f = m$ and $\tilde{g}_{bb} = 0.5$.

Fig. 7. The same as in fig. 6, but for a disk-shaped trap with $\lambda = 2.0$.

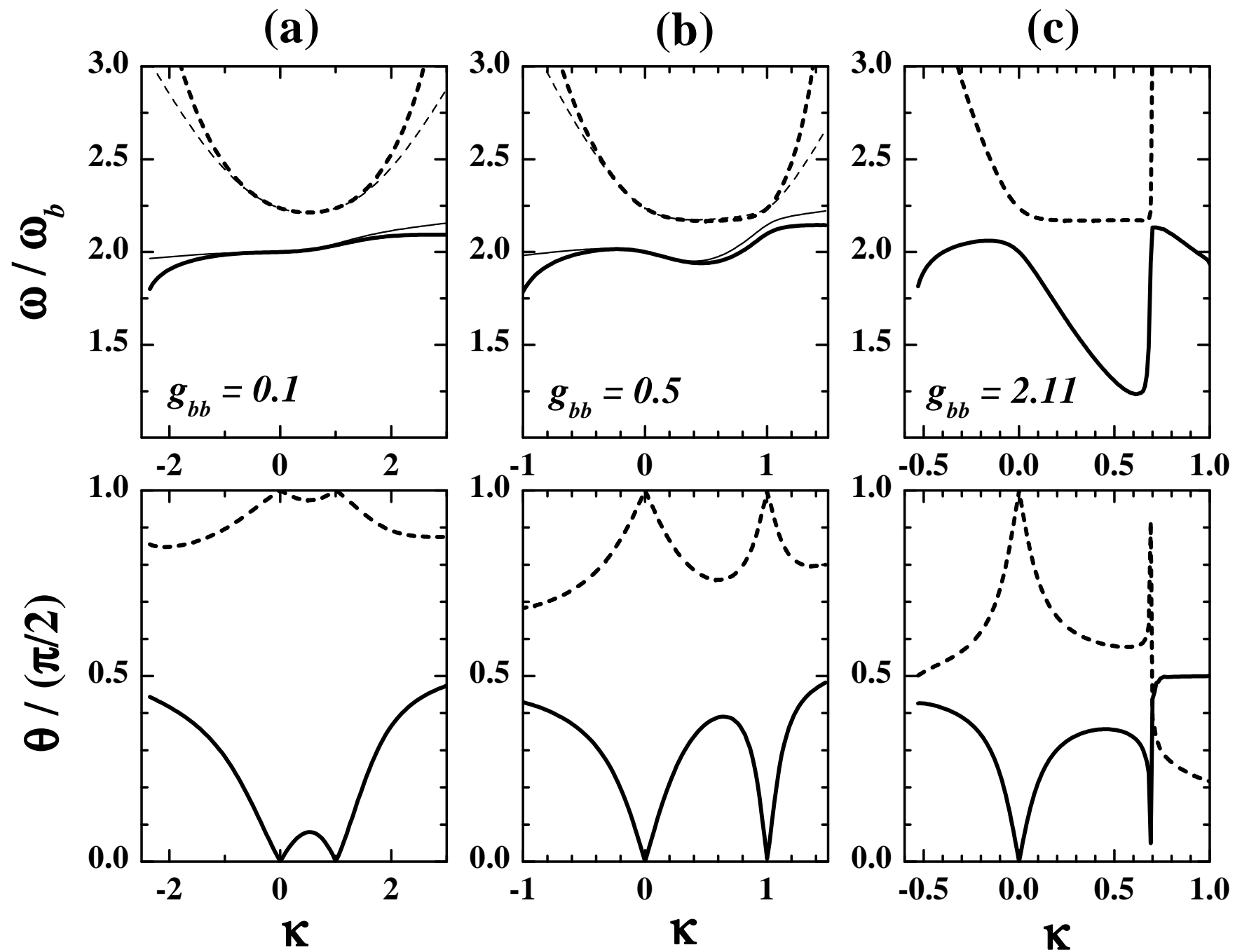


Figure 1, X. Liu *et al.*,

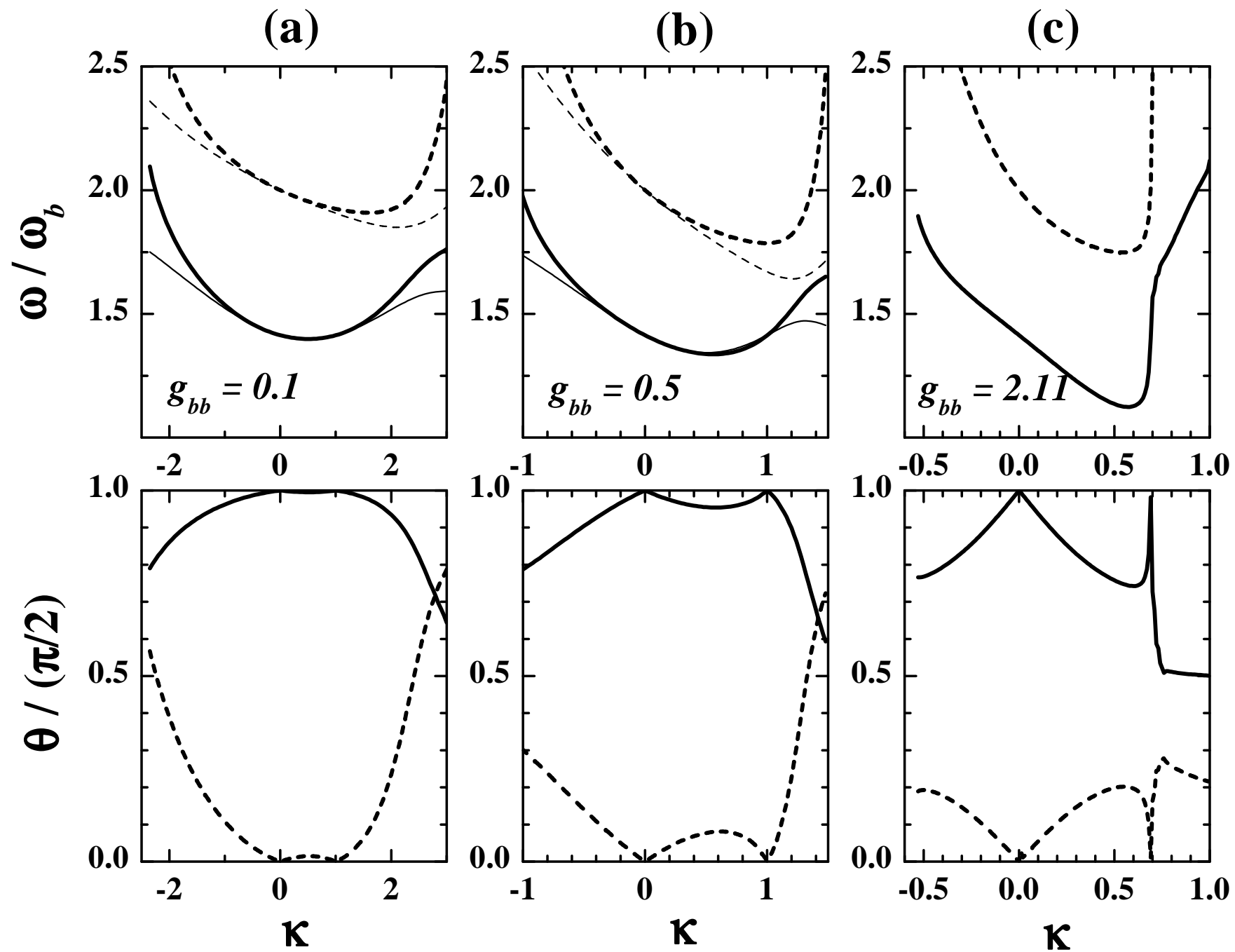


Figure 2, X. Liu *et al.*,

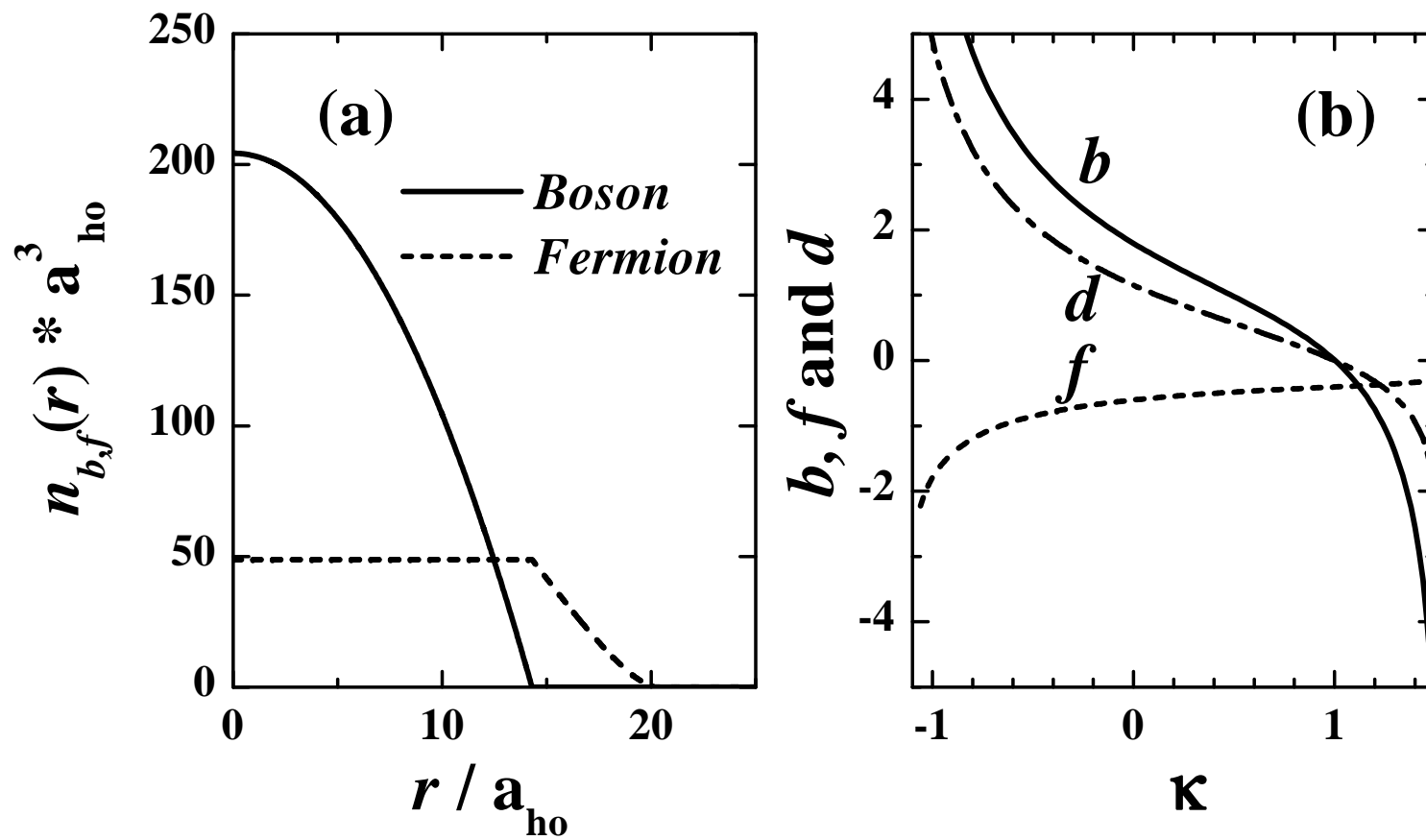


Figure 3, X. Liu *et al.*,

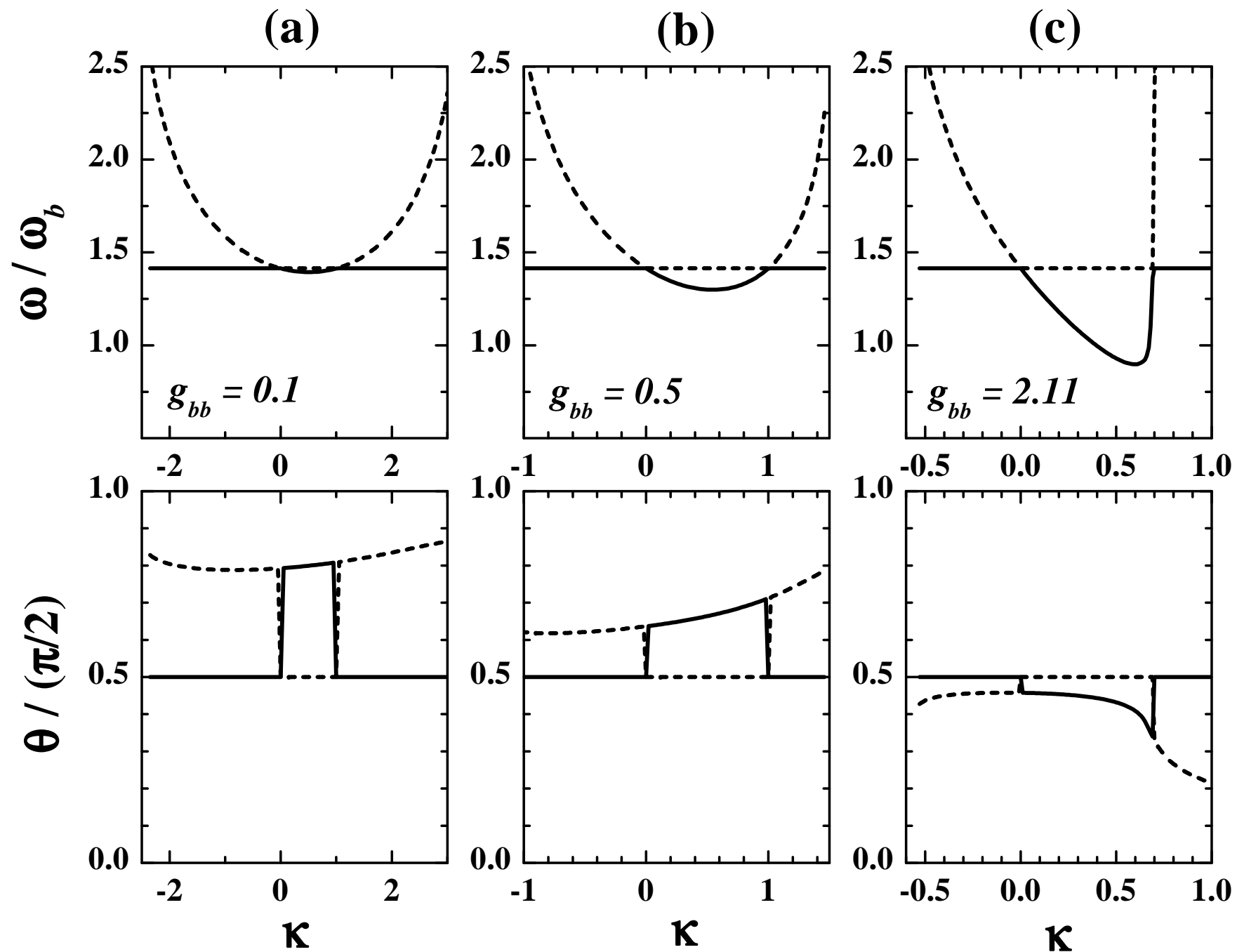


Figure 4, X. Liu *et al.*,

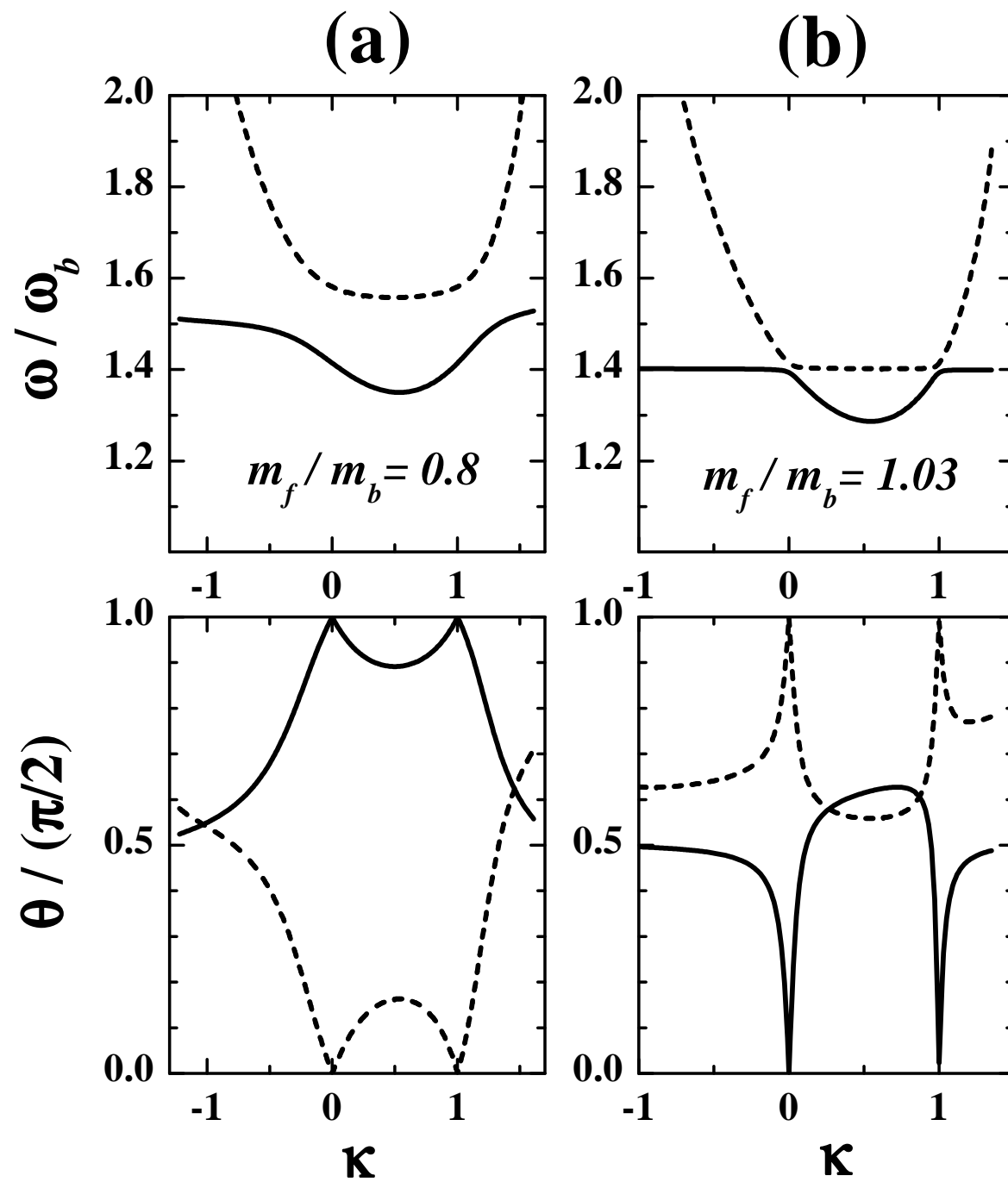


Figure 5, X. Liu *et al.*,

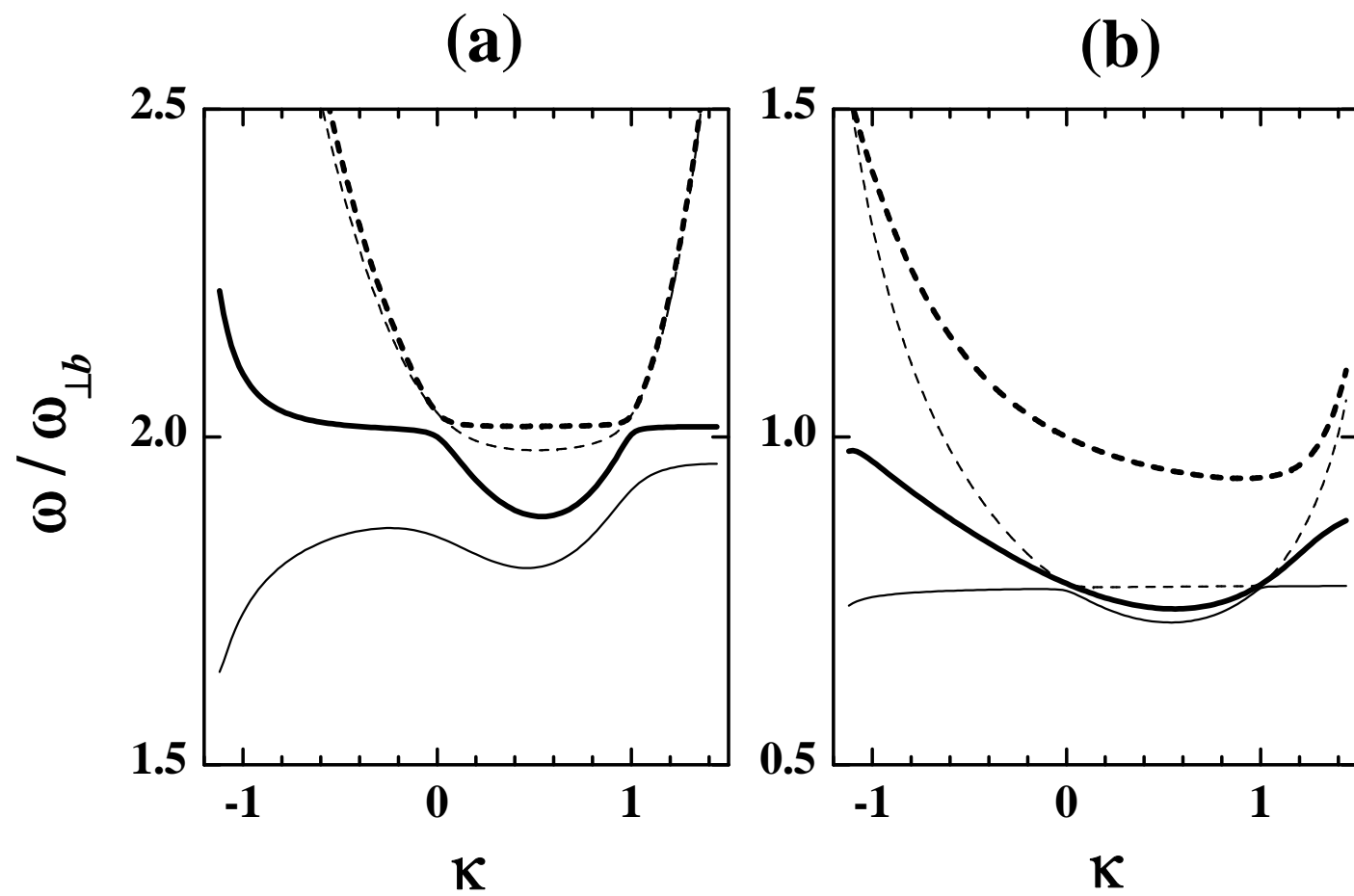


Figure 6, X. Liu *et al.*,

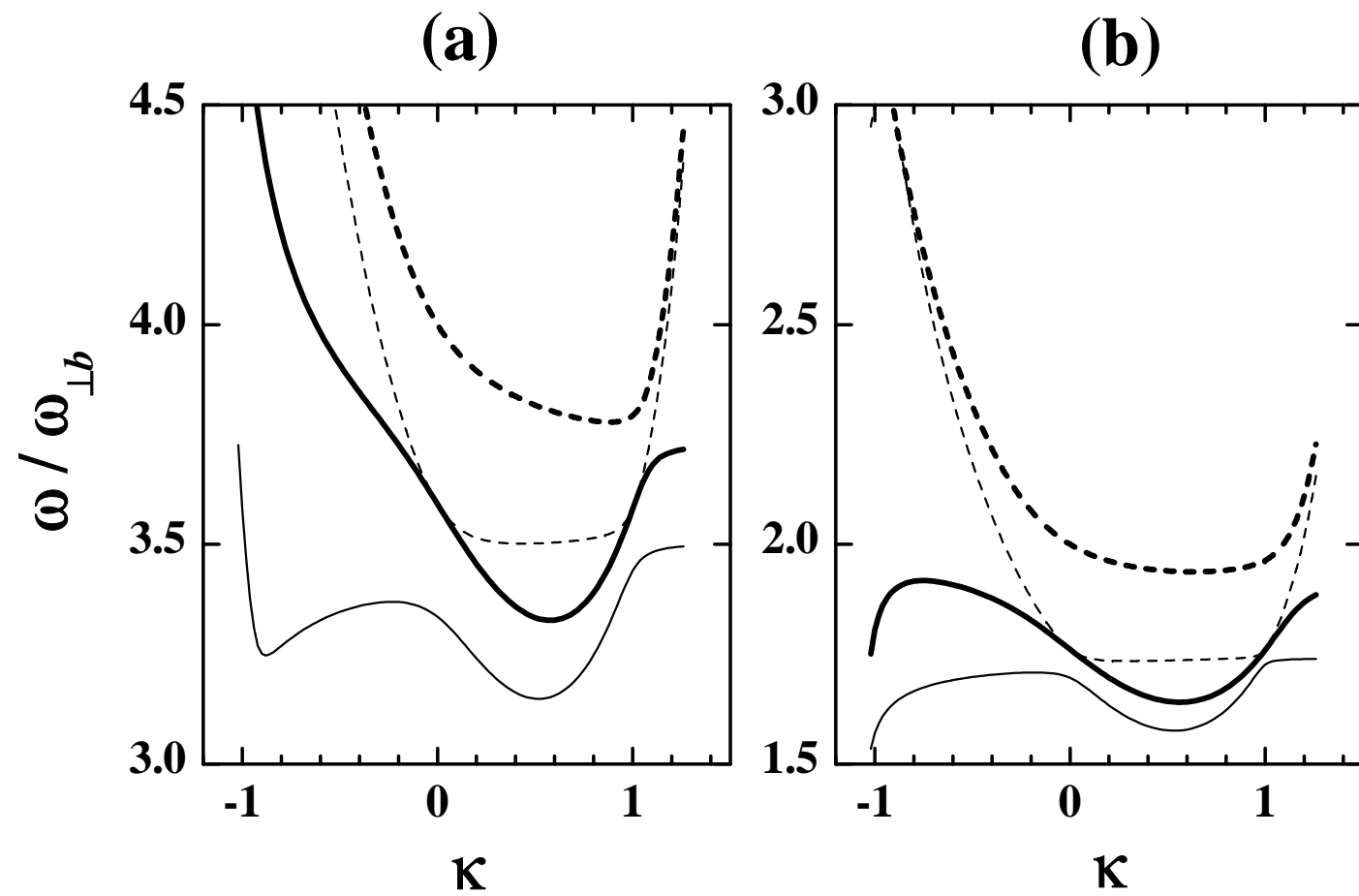


Figure 7, X. Liu *et al.*,